Gas Processing Journal
Vol. 4, No. 1, 2016
http://gpj.ui.ac.ir

Positive Coupling Effect in Gas Condensate Flow Capillary Number Versus Weber Number

Mohammad Mohammadi-Khanaposhtani*

Faculty of Fouman, College of Engineering, University of Tehran, Fouman, Iran

Article History
Received: 2015-10-15 Revised: 2016-10-17 Accepted: 2016-11-01

Abstract
Positive coupling effect in gas condensate reservoirs is assessed through a pure theoretical approach. A combination of linear stability analysis and long bubble approximation is applied to describe gas condensate coupled flow and relative permeability, thereof. The role of capillary number in gas condensate flow is clearly expressed through closed formula for relative permeability. While the model is intended to give a clear image of positive coupling through comprehensible fluid mechanical arguments, it predicts relative permeability values that are not too far from limited published experimental data presented in the literature. Based on the systematic deviation of the model results from experimental data, it could be expected to serve as a basis for generalized gas condensate relative permeability correlations by including inertial effects in terms of Weber number as discussed in this study. The success of this theoretical approach in describing the role of capillary number and Weber number on gas condensate relative permeability motivates further study of the underlying mechanism of flow coupling in near well-bore region of gas condensate reservoirs in the hope of pure theoretical and yet predictive equations for gas condensate relative permeability.

Keywords
Rlative Permeability, Gas Condensate, Positive Coupling Effect, Capillary Number, Weber Number

1. Introduction

The near wellbore behavior of gas condensate reservoir has been and is subject to intensive studies for the past two decades and it is assumed that it will remain as an active research area in this decade as well (Azamifard, Hekmatzadeh, & Dabir, 2016; Haji Seyedi, Jamshidi, & Masihi, 2014; Nasriani, Borazjani, Iraji, & Moradi Dowlat Abad, 2015; Rahimzadeh, Bazargan, Darvishi, & Mohammadi, 2016). Henderson et al. (1995) revealed that in low interfacial tension (IFT) an increase in velocity of gas condensate flow may lead to an increase in both phases' relative permeability (G. D. Henderson, Danesh, Tehrani, & Peden, 1997). They named this velocity effect as 'positive coupling effect'. Later, it was revealed that the relative permeability data of low IFT gas condensate flow is strongly related to capillary number (Blom & Hagoort, 1998; G. Henderson, Danesh, Tehrani, Al-Shaidi, & Peden, 1996; Shaidi, 1997). Capillary number is the viscous force to capillary resistance dimensionless ratio, Eq. (2). Hence, an increase in velocity and/or a decrease in IFT are expected to increase gas/condensate relative permeability, even in the absence of strong inertial effects. While the effect of IFT is clearly understood in terms of basic concepts of relative permeability, the positive effect of velocity on relative permeability cannot be described in Darcy's law frame or its modified form (i.e. the Forchheimer equation). Jamiolahmady et al. (2000) presented the first theoretical study on the positive coupling effect (M Jamiolahmady, Danesh, Tehrani, & Duncan, 2000). They developed a coupled flow model based on liquid-film instability in a constricted capillary

* Corresponding Author.
Authors' Email Address:
Mohammad Mohammadi-Khanaposhtani (muhammadi_mu@ut.ac.ir),
ISSN (Online): 2345-4172, ISSN (Print): 2322-3251

(Gauglitz & Radke, 1990) to describe the positive effect of velocity on gas and condensate relative permeabilities. They concluded that there exists a fundamental relation between gas-condensate relative permeability and the phase's flow fraction instead of their saturation. Later, it was observed that expressing gas condensate relative permeability as a function of flow fraction (instead of saturation) minimizes the rock type effects on relative permeability (M Jamiolahmady, Sohrabi, Ireland, & Ghahri, 2009). Following this, in their generalized correlation, Jamiolahmady et al. (2009) presented gas condensate relative permeability in terms of condensate to gas volumetric flow rate ratio (CGR). In this correlation, both capillary number and gas phase inertial factor are included to treat coupling and inertia, respectively (Mahmoud Jamiolahmady, Sohrabi, Ghahri, & Ireland, 2010; M Jamiolahmady et al., 2009).
Mohammadi-Khanaposhtani et al. (Mohammadi-Khanaposhtani, Bahramian, & Pourafshary, 2014) combined the effect of viscous force and capillary resistance with disjoining pressure (Derjaguin, 1939), (excess film pressure arising from van der Waals molecular interactions) to determine the pressure drop in gas condensate coupled flow. They applied this pure theoretical pressure drop for calculating relative permeability as a function of capillary number and Scheludko number (the disjoining pressure to capillary resistance dimensionless ratio) in a single cylindrical pore. The positive velocity effect on gas condensate relative permeability predicted through this model provided that low values of Scheludko number are coupled with large values of capillary number. That the relative permeability in the coupled flow regime is a function of flow fraction rather than fluid saturation is revealed in this theoretical model. (Mohammadi-Khanaposhtani et al., 2014) calculated the minimum flow fraction for coupling in a straight cylindrical pore without directly expressing the relative permeability as a function of flow fraction in their model. They did not include the negative inertial effect on relative permeability either. Attempt is made in this study to derive a relative permeability expression for the coupled flow in terms of condensate flow fraction. The role of capillary number is determined by Bretherton's long bubble approximation (Bretherton, 1961) and the flow fraction is included through material balance arguments together with a modified version of Hagen-Poiseuille equation. The yield expression is a closed formula for gas and condensate relative permeability that gives a clear picture of what the contributive capillary number and flow fraction is in gas condensate flow. The predicted values of relative permeability by this pure theoretical formula do not match the experimental data, while as limited data available, it is observed that the deviation between model prediction and experiment can be described by replacing the model constant with a function of Weber number (the inertial force to capillary resistance dimensionless ratio, Eq. (18)). The result here indicates a new basis for a generalized correlation for gas condensate relative permeability that only applies the routine core analysis data (absolute permeability and porosity) and fluid properties (IFT and density).

2. Model Description

The coupled flow of gas and condensate is considered as a steady flow of gas bubbles with condensate slugs between them. The condensate slugs look like concave lenses and the difference between curvatures of the two sides of a lens determines the pressure drop per lens (or equivalently per gas bubble). For high liquid fractions the viscous resistance of the wall against liquid flow must be considered in calculating the total pressure drop. This flow regime is introduced as the'train of gas bubbles' by Ratulowski and Chang (1989) and is adopted in assessing the apparent viscosity in foam flooding (Ratulowski & Chang, 1989). This model requires prior knowledge of the number of bubbles for specifying total pressure drop and relative permeability. An estimation of the number of bubbles with linear stability theory is possible in a straight capillary tube, applied in estimating the total pressure drop and relative permeability as discussed in this section.

2.1. Pressure Drop

The coupled flow in microchannel is associated with formation of long bubbles (Kawahara, Chung, & Kawaji, 2002) and the sum of pressure drop across bubbles is the total pressure drop. At low velocities, a single bubble's pressure drop (ΔP_b) could be estimated with Bretherton's long bubble approximation (Bretherton, 1961) as:

$$\Delta P_b = 9.40 N_{ca}^{2/3} \frac{\sigma}{R} \quad (1)$$

where, σ is the interfacial tension and R is the radius of the cylindrical pore. The capillary, N_{ca} number and it is defined as:

$$N_{ca} = \frac{\mu_c U}{\sigma} \quad (2)$$

where, μ_c is the condensate viscosity and U is the velocity of the coupled flow yield by dividing total volumetric flow rate of gas and condensate by the active cross sectional area as presented by Eq.3:

$$U = \frac{Q_{tot}}{A\phi}\left(\frac{R}{R_i}\right)^2 \quad (3)$$

It should be noted that due to presence of a deposited condensate film on the channel wall, the total cross sectional area of the channel is not accessible to the coupled flow. The thickness of the deposited film on the pore wall (H_i) is estimated according to (Bretherton, 1961)

$$\frac{H_i}{R} = 1.338 N_{ca}^{2/3} \quad (4)$$

hence, the effective radius of the channel for the coupled flow is:

$$R_i = R - H_i \quad (5)$$

The total pressure drop in this model is obtained by multiplying the number of bubbles (N_b) by a single bubble's pressure drop (ΔP_b).

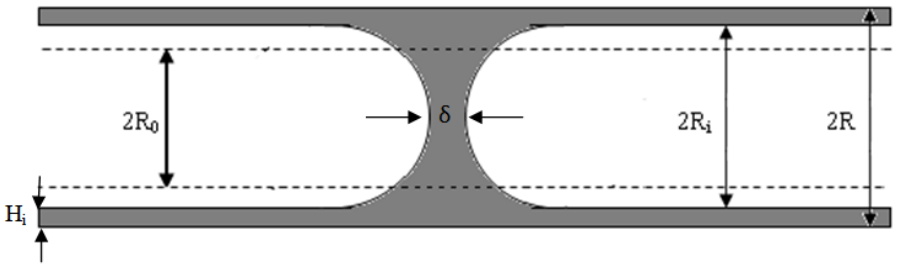

Figure 1. Schematic Diagram of Condensate Lens and the Deposited Film in a Cylindrical Pore

For the high liquid fractions, the pressure drop due to viscous nature of the wall against liquid flow must be added to the bubble pressure drop. The liquid slug pressure drop is estimated with a modified version of Hagen-Poiseuille equation. Determining the actual value of N_b - even in channels with the simplest geometry requires experimental observations. Attempt is made here to estimate the number of bubbles through linear film stability theory (Hammond, 1983). It is assumed that lens formation is a result of instability of a thick liquid film of undisturbed radius R_0 within a cylindrical channel (Fig. 1). Note that the condensate flow fraction is in relation to R_0 and R_i as:

$$f_c = \frac{\pi\left(R_i^2 - R_0^2\right)L}{\pi R_i^2 L} = 1 - \frac{R_0^2}{R_i^2} \quad (6)$$

where, R_0 is the initial film radius. Now, assume that liquid lenses are formed at equal distances λ, which might be named the 'prevailing disturbance wavelength'. It is obvious that number of bubbles formed in a capillary of length L is obtained through Eq. (7):

$$N_b = \frac{L}{\lambda} \quad (7)$$

For bubble formation, a wavelength must contain enough liquid to provide a deposited film of thickness H_i and a lens of thickness δ and radius R_i. Following this discussion a material balance equation is written to find the volume of a lens (V_l) through:

$$V_l = \pi\left(R_i^2 - R_0^2\right)\lambda = \pi R_i^2\left(2R_i + \delta\right) - \frac{4}{3}\pi R_i^3 \quad (8)$$

By combining Eqs. (6 and 8) one can determine the thickness of the liquid lens through:

$$\delta = \lambda f_c - \frac{2}{3}R_i \quad (9)$$

Since total flow rate is known, R_i is determined Through Eqs. (3 to 5). The flow fraction is treated as an independent variable as well, hence, if the prevailing wavelength is known, the thickness of the lens and the number of bubbles are determined in a straight forward manner. According to linear stability theory (Hammond, 1983), for thin liquid films on the inner wall of a cylindrical capillary, the fastest growing disturbances have a wavelength of

$\lambda = 2\sqrt{2}\pi R_0$. Assuming this wavelength to be the prevailing wavelength we can determine the number of bubbles and lens thickness through:

$$N_b = \frac{L}{2\sqrt{2}\pi R_0} \tag{10a}$$

$$\delta = 2\sqrt{2}\pi R_0 f_c - \frac{2}{3}R_i \tag{10b}$$

An immediate result of equation (10b) is the minimum condensate flow fraction for coupled gas condensate flow which is determined as $f_c^{\min} = 0.0781$. This result follows from substitution of R_0/R_i from (6) with Eq. (10b) and setting $\delta = 0$ in the latter. Note that the assumption of $\lambda = 2\sqrt{2}\pi R_0$ remains valid until the predicted bubble length becomes greater than $2R_i$ because a smaller bubble cannot be formed in microchannels due to weakness of shear forces against surface force (Griffith & Lee, 1964; Kawahara et al., 2002). In this case one can assume a fixed bubble length of $2R_i$ and a change in lens thickness to meet the conditions in material balance equation, (Eq. (8)). In mathematical context, the range of validity of this assumption on prevailing wavelength is limited to $\delta \le 2\sqrt{2}\pi R_0 - 2R_i$ and through Eq. (10b) Eq. (11) is yield:

$$2\sqrt{2}\pi\left(1-f_c\right)^{3/2} - \frac{4}{3} = 0 \;\rightarrow\; f_c^{\max} = 0.7176 \tag{11}$$

For greater condensate flow fraction the assumption of $\lambda = 2\sqrt{2}\pi R_0$ cannot be applied while a unique value for λ can be determined according to material balance equation and minimum bubble size requirement. For low condensate fractions, the viscous pressure drop is usually negligible compared to the bubbles' pressure drop. Here, for high condensate flow fractions or highly viscous liquid phase one should consider the viscous pressure drop, which could becomes possible by a modified version of Hagen-Poiseuille equation as:

$$\Delta P_s = \frac{8\mu UL}{R_i^2} f_c \tag{12}$$

where, ΔP_s is the slug pressure drop due to viscous resistance, consequently, the total pressure drop is expressed as:

$$\Delta P_{tot} = N_b \Delta P_b + \Delta P_s \tag{13}$$

By knowing the total pressure drop one can determine the relative permeability of the gas and condensate.

2.2. Relative Permeability

In coupled flow regime both the gas and condensate experience a common pressure drop of (ΔP_{tot}) and the relative permeability according to Darcy law expressed through:

$$k_{rc} = \frac{\mu_c f_c Q_{tot}}{kA\left(\Delta P_{tot}/L\right)} \tag{14a}$$

$$k_{rg} = \frac{\mu_g \left(1-f_c\right) Q_{tot}}{kA\left(\Delta P_{tot}/L\right)} \tag{14b}$$

Now by assuming the viscous flow and replacing the pore with a cylindrical capillary, the absolute permeability is expressed through Hagen-Poiseuille equation as

$$k = \frac{\phi R^2}{8} \tag{15}$$

Rearranging equation (14) and applying equations (15) the relative permeability of each phase is expressed through:

$$k_{rc} = \frac{8\mu_c\left(Q^{tot}/A\phi\right)}{R^2\left(\Delta P_{tot}/L\right)} f_c = \frac{8N_{ca}}{\left(1+1.338N_{ca}^{2/3}\right)^4\left(1.0579\frac{N_{ca}^{2/3}}{f_c\sqrt{1-f_c}}+8N_{ca}\right)} \tag{16a}$$

$$k_{rg} = \frac{\mu_g\left(1-f_c\right)}{\mu_c f_c} k_{rc} \tag{16b}$$

where N_{ca} is too small, Eq. (16) is simplified into:

$$k_{rc} = 7.56 N_{ca}^{1/3} \frac{CGR}{\left(1+CGR\right)^{3/2}} \tag{17a}$$

$$k_{rg} = 7.56 N_{ca}^{1/3} \frac{\mu_g/\mu_c}{\left(1+CGR\right)^{3/2}} \tag{17b}$$

where, $CGR = f_c/\left(1-f_c\right)$ is the condensate to gas ratio. The positive role of capillary number on both the gas and condensate relative permeability is expressed in Eq. (17). Note that this simplification amounts to neglecting both slug viscous resistance and the reduction of flow area due to presence of the deposited condensate film. As observed in figure 2 this assumption is accepted for $N_{ca} < 10^{-4}$.

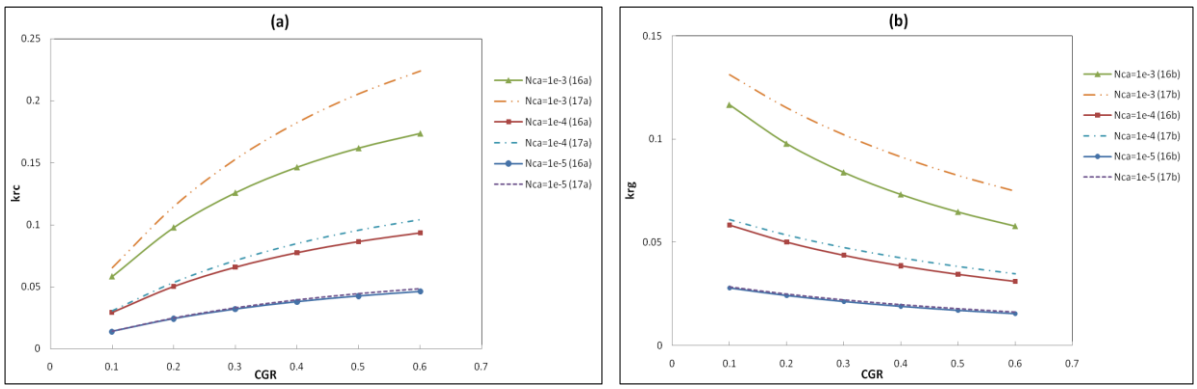

Fugure 2. Predicted Condensate Relative Permeability (a) and Gas Relative Permeability (b) as a Function of Condensate to Gas Ratio for $\mu_g = 0.2\mu_c$

As predicted through this model, at any flow fraction, an increase in capillary number always enhances the flow of both phases, that is, the positive effect of velocity on gas condensate relative permeability which is in accordance with the experimental observations at low IFT and weak inertial effect. In the next section we make a quantitative comparison between the model and to our knowledge the only available flow-fraction based steady state gas condensate relative permeability data in the literature. The limitations of this model in prediction of relative permeability of low IFT gas condensate flow is determined through these comparisons which would contribute in suggesting strategies to overcome these limitations.

3. Comparison with Experimental Data

For evaluation of this proposed model the gas condensate relative permeability data presented as a function of condensate flow fraction is of essence. Gas and condensate viscosities must be provided and the data should be obtained from steady state tests as discussed by Henderson et al. (G. Henderson et al., 1996). To the best of the authors knowledge such datawas presented by (M Jamiolahmady et al., 2009). The core applied in the aforementioned experiment has 6% porosity and 3.9 mD absolute permeability. Hence, by applying Eq. (15) the characteristic channel radius is found to be 0.72 microns. Fluid properties are tabulated in Table 1 and the calculated capillary number and Weber number are tabulated in Table 2. Weber number is the dimensionless inertia to capillary resistance ratio, expressed through:

$$N_{Wb} = \frac{\rho_g U^2 d}{\sigma} \tag{18}$$

Figure 3 compares the model prediction with experimental data for IFT of 0.85mNm^{-1} Is compared in Fig. (3)

Table 1. Fluid Properties in Jamiolahmady et al. (2009) (M Jamiolahmady et al., 2009)

Test No.	1	2	3
IFT (mNm^{-1})	0.85	0.15	0.036
μ_c (cp)	0.0601	0.0474	0.0405
μ_g (cp)	0.0172	0.0206	0.0249
ρ_c (kgm^{-3})	404	345.1	317.4
ρ_g (kgm^{-3})	132.6	184.8	211.4

Table 2. Calculated Capillary Number and Weber Number for Different Tests

IFT (mNm^{-1}) / Velocity (md^{-1})	0.85		0.15		0.036	
	$N_{ca}\times10^4$	$N_{Wb}\times10^6$	$N_{ca}\times10^4$	$N_{Wb}\times10^6$	$N_{ca}\times10^4$	$N_{Wb}\times10^6$
4.6	—	—	—	—	0.601	
22.8	0.187	0.0156	0.838	0.124	3.00	0.589
45.7	0.375	0.0628	1.68	0.496	6.05	2.37
91.3	0.751	0.251	3.38	1.98	12.2	9.44
182.6	1.51	1.00	6.82	7.92	—	—

A change in the observed gas relative permeability trend as CGR increases from 0.005 to 0.03, Fig. (3b), indicating a transition in flow regime - literally from annular flow to slug flow. After this transition the coupled flow is assured by the observed positive effect of velocity. Here, at IFT of 0.85mNm^{-1} the predicted and observed trends match. As observed in Fig. (3) the model does not predict the correct values of relative permeability is not predicted by this model, instead; a somewhat uniform deviation is observed between model and data with model predictions about 3 times smaller than the experimental values. The positive velocity effect between the high velocities, (i.e. 91.3 and 182.6 md^{-1}), is not as pronounced as other cases. This weakness can be attributed to the increase in Weber number, (i.e. strength of inertial effects at higher velocities). At IFT of 0.15 mNm^{-1}, the inertial effect becomes dominant at higher velocities as observed in Fig. 4, where, the velocity effect is no longer monotonic and the predicted (positive) trend is only observed between the lower velocities, (i.e. 22.8 and 45.7 md^{-1}).

Note that the strength of inertial effects is not merely due to an increase in flow velocity. Smaller IFT's increase both the capillary number and Weber number, that is, as IFT decreases, the Weber number may increase in a manner that the resultant inertia could not be compensated by an increase in capillary number. Accordingly, the push-pull effect of IFT must be well understood for describing the effect of velocity on gas condensate relative permeability. However, in brief one can claim that low IFT is necessary for positive coupling appearance but when IFT becomes too low, it favors inertia as observed by making a comparison between Fig. (3 and 4).

As to the model, it is observed that the predicted values in Fig. 4 are smaller than that of the experimental data by a deviation factor between 1.8 and 4.2, which is no longer a constant but a decreasing function of the velocity. At low IFT of 0.036mNm^{-1} the inertial effect dominates the positive coupling effect completely (Fig. 5), making the model fail to predict the right trend.

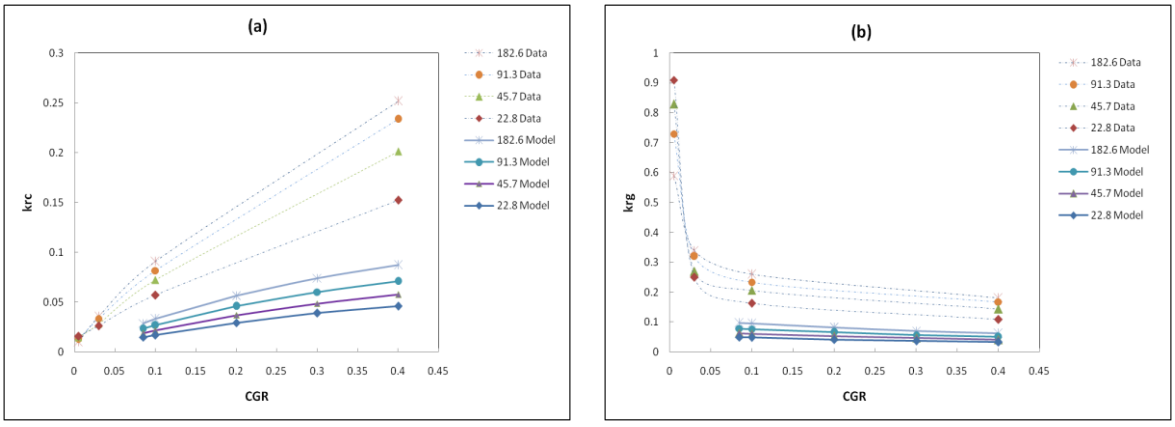

Figure 3. Comparison of Model with Experimental Data (from Jamiolahmady et al. 2009 (M Jamiolahmady et al., 2009)) for IFT=0.85mNm^{-1}; the Predicted Values Deviate by an Almost Constant Factor

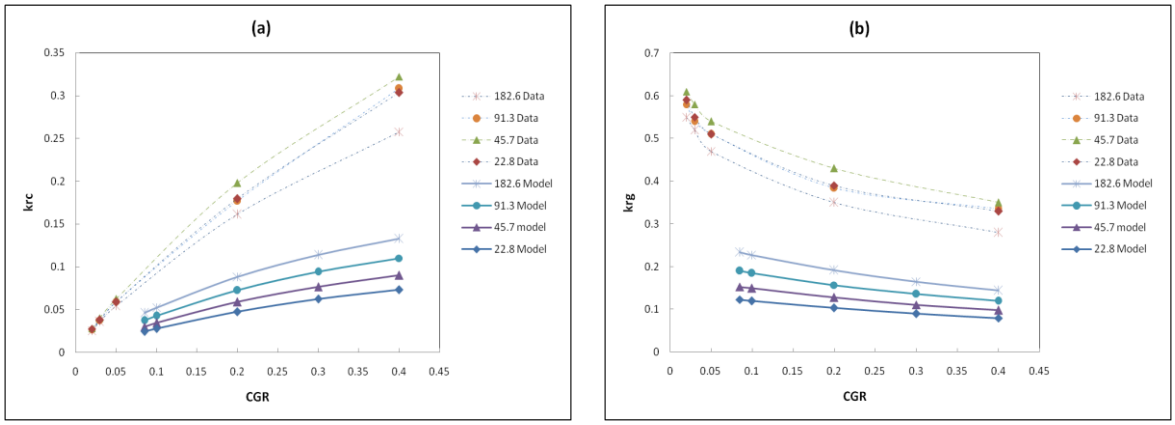

Figure 4. Comparison of Model with Experimental Data (from Jamiolahmady et al. 2009 (M Jamiolahmady et al., 2009)) for IFT=0.15mNm^{-1}; Predicted Values Deviate by a Factor b/w 1.8 and 4.2

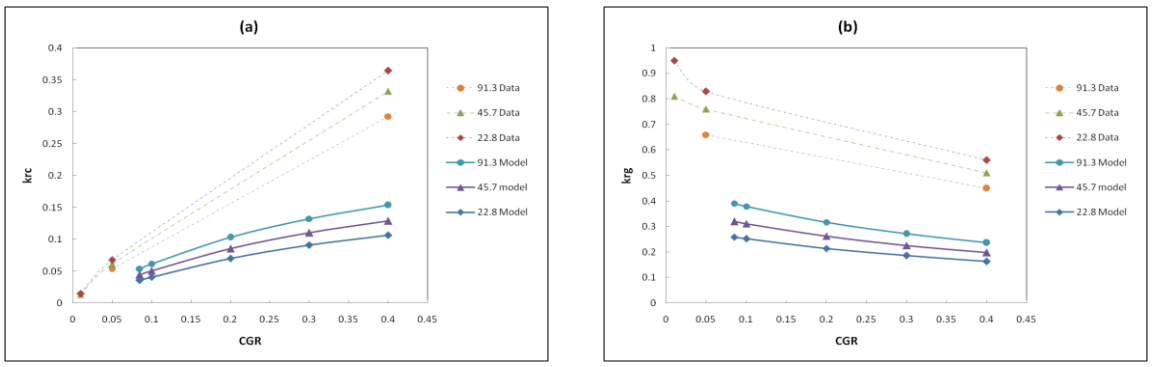

Figure 5. Comparison of Model with Experimental Data (from Jamiolahmady et al. 2009 (M Jamiolahmady et al., 2009)) for IFT=0.15mNm^{-1}; Predicted Values Deviate by a Factor b/w 1.9 and 3.4

When, the predicted trend is not right, due to dominant inertial effect, the predicted values deviate from the experimental values by a deviation factor within 1.9 to 3.4 ranges, once more indicating that the deviation factor is a decreasing function of velocity.

4. Discussion

The upper limit of IFT where positive coupling can take place is experimentally determined to be 3mNm^{-1} by Jamiolahmady et al. (2009) (M Jamiolahmady et al., 2009), while at very low IFT, the positive effect of velocity is dominated by negative inertial effect. Now if the predicting trend is right in velocity-IFT plane the positive coupling effect is expected and this proposed model would predict the right trend in this region in a qualitative manner. The wrong place for the model is where inertia dominates positive coupling effect; more precisely, when the Weber number is large enough (due to very low IFT or very high velocity) an increase in capillary number can no longer regenerate the positive coupling effect. For the experimental data available $N_{Wb} \geq 10^{-6}$ is suggested for domination of inertial effects.

Whether positive coupling is dominant or is dominated, the predicted values of relative permeability by this pure theoretical model are not too far from the observed values; in general they are smaller than the experimental data by a factor within 1.8 and 4.2 ranges. Moreover, almost in all cases the deviation factor decreases as velocity increases (figure 6).

The deviation factor as a function of Weber number is shown in Fig. (7). The curves related to the lower IFT values overlap in this figure (i.e. the deviation factor for both cases is a unique function of the Weber number). This idea is encouraging for devising a relative permeability correlation based on this proposed model where Eq. (16) is modified by a factor depending on the Weber number. This modification allows accounting for the inertia as well coupling in the resulting correlation. For a moment the equation of overlapping curves in Fig. (7), ($DF = 0.227 N_{Wb}^{-0.18}$; $R^2 = 0.986$) is taken into account, then the hypothetical generalized correlation is expressed as:

(19)

$$k_{rc} = \frac{1.816 N_{Wb}^{-0.18} N_{ca}}{\left(1+1.338 N_{ca}^{2/3}\right)^4 \left(1.0579 \frac{N_{ca}^{2/3}}{f_c\sqrt{1-f_c}} + 8 N_{ca}\right)}$$

Of course extensive data is necessary to check the plausibility of such a generalized correlation.

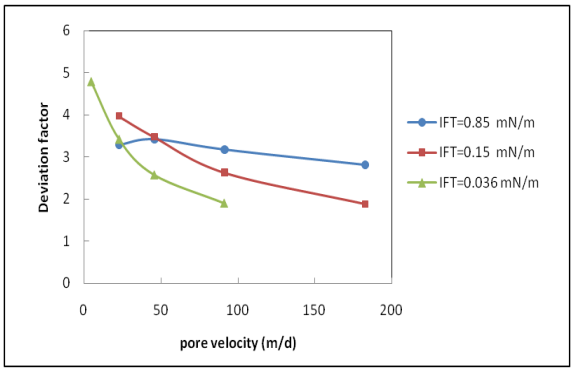

Figure 6. Deviation Factor as a Function Pore Velocity for Different Values of IFT

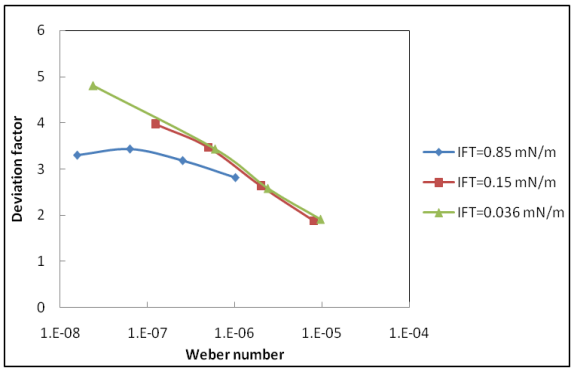

Figure 7. Deviation Factor as a Function Pore Velocity for Different Values of IFT

5. Conclusion

The coupled flow of gas and condensate is a result of formation of condensate slugs (or lenses) that bridge across the pore. These lenses move with the gas phase in a manner that is best phrased as "train of gas bubbles". In this study, by assuming cylindrical pores, the coupled flow pressure drop is estimated by combining linear stability analysis and Bretherton's long bubble approximation. The result is then up scaled to core level by bundle of capillary tubes (BCT) approach. Application of BCT model is justified by expressing relative permeability as a function of *flow fraction* rather than *saturation*, because flow fraction can integrate between relative permeability data of different cores. The main results obtained through this study could be listed as follows:

- This proposed model, based on comprehensible fluid mechanical arguments, clearly indicates how an increase in capillary number can positively affect gas and condensate relative permeability
- A comparison with experimental data reveals that the model predicts the right trend at low values of the Weber number (i.e. in the absence of dominant inertial effects). At too low IFT's the flow becomes wettability controlled and the model cannot predict the right trend in the full span of flow velocity
- For the limited experimental data available, the predicted values by the model are always smaller than the experimental values by a factor within 1.8 and 4.2 ranges. At low IFT's the deviation from experimental data can be expressed by a unique function of the Weber number. At high IFT, where inertia is dominated by capillary resistance, the deviation does not follow the same trend as in low IFT's and the deviation factor seems to remain constant.

According to these results, this theoretical model suggests a new manner of correlating gas condensate relative permeability data based on capillary number and the Weber number. Introducing a predictive correlation based on this model requires extensive experimental data and a deeper understanding of the underlying physics of the phenomena. This pure theoretical model on its own describes how positive coupling takes place at pore level and it reveals the promising role of the Weber number (and not just capillary number) in low IFT gas condensate flow.

References

Azamifard, A., Hekmatzadeh, M., & Dabir, B. (2016). Evaluation of gas condensate reservoir behavior using velocity dependent relative permeability during the numerical well test analysis. *Petroleum, 2*(2), 156-165. doi: http://dx.doi.org/10.1016/j.petlm.2016.02.005

Blom, S., & Hagoort, J. (1998). *How to include the capillary number in gas condensate relative permeability functions?* Paper presented at the SPE Annual Technical Conference and Exhibition.

Bretherton, F. (1961). The motion of long bubbles in tubes. *Journal of Fluid Mechanics, 10*(02), 166-188.

Derjaguin, B. (1939). Anomalous properties of thin polymolecular films. *Acta Phys. Chim, 10*, 253.

Gauglitz, P. A., & Radke, C. J. (1990). The dynamics of liquid film breakup in constricted cylindrical capillaries. *Journal of Colloid and Interface Science, 134*(1), 14-40. doi: http://dx.doi.org/10.1016/0021-9797(90)90248-M

Griffith, P., & Lee, K. S. (1964). The Stability of an Annulus of Liquid in a Tube. *Journal of Basic Engineering, 86*(4), 666-668.

Haji Seyedi, S. H., Jamshidi, S., & Masihi, M. (2014). A novel method for prediction of parameters of naturally fractured condensate reservoirs using pressure response analysis. *Journal of Natural Gas Science and Engineering, 19*, 13-22. doi: http://dx.doi.org/10.1016/j.jngse.2014.04.010

Hammond, P. (1983). Nonlinear adjustment of a thin annular film of viscous fluid surrounding a thread of another within a circular cylindrical pipe. *Journal of Fluid Mechanics, 137*, 363-384.

Henderson, G., Danesh, A., Tehrani, D., Al-Shaidi, S., & Peden, J. (1996). Measurement and correlation of gas condensate relative permeability by the steady-state method. *SPE Journal, 1*(02), 191-202.

Henderson, G. D., Danesh, A., Tehrani, D. H., & Peden, J. M. (1997). The effect of velocity and interfacial tension on relative permeability of gas condensate fluids in the wellbore region. *Journal of Petroleum Science and Engineering,*

17(3), 265-273. doi: http://dx.doi.org/10.1016/S0920-4105(96)00048-4

Jamiolahmady, M., Danesh, A., Tehrani, D., & Duncan, D. (2000). A mechanistic model of gas-condensate flow in pores. *Transport in porous media, 41*(1), 17-46.

Jamiolahmady, M., Sohrabi, M., Ghahri, P., & Ireland, S. (2010). Gas/condensate relative permeability of a low permeability core: coupling vs. inertia. *SPE Reservoir Evaluation & Engineering, 13*(02), 214-227.

Jamiolahmady, M., Sohrabi, M., Ireland, S., & Ghahri, P. (2009). A generalized correlation for predicting gas–condensate relative permeability at near wellbore conditions. *Journal of Petroleum Science and Engineering, 66*(3), 98-110.

Kawahara, A., Chung, P.-Y., & Kawaji, M. (2002). Investigation of two-phase flow pattern, void fraction and pressure drop in a microchannel. *International Journal of Multiphase Flow, 28*(9), 1411-1435.

Mohammadi-Khanaposhtani, M., Bahramian, A., & Pourafshary, P. (2014). Disjoining pressure and gas condensate coupling in gas condensate reservoirs. *Journal of Energy Resources Technology, 136*(4), 042911.

Nasriani, H. R., Borazjani, A. A., Iraji, B., & MoradiDowlatAbad, M. (2015). Investigation into the effect of capillary number on productivity of a lean gas condensate reservoir. *Journal of Petroleum Science and Engineering, 135*, 384-390. doi: http://dx.doi.org/10.1016/j.petrol.2015.09.030

Rahimzadeh, A., Bazargan, M., Darvishi, R., & Mohammadi, A. H. (2016). Condensate blockage study in gas condensate reservoir. *Journal of Natural Gas Science and Engineering, 33*, 634-643. doi: http://dx.doi.org/ 10.1016/j.jngse.2016.05.048

Ratulowski, J., & Chang, H. C. (1989). Transport of gas bubbles in capillaries. *Physics of Fluids A: Fluid Dynamics, 1*(10), 1642-1655.

Shaidi, S. M. A. (1997). *Modelling of gas-condensate flow in reservoir at near wellbore conditions.* Heriot-Watt University.

Nomenclature

English letters

A	Cross sectional area of the pore
CGR	Condensate to gas volumetric flow ratio
DF	Deviation factor
f_c	Condensate Flow fraction
H	Film thickness
K	Permeability
L	Length of capillary tube
m	Viscosity ratio
N_{ca}	Capillary number
N_{Wb}	Weber number
P	Pressure
Q_{tot}	Total volumetric flow rate
R	Radius of cylindrical pore
R_i	Radius of film interface
R_0	Initial Radius of film interface
U	Velocity of the coupled flow
V_l	Volume of the lens
x	Axial coordinate
y	Vertical coordinate

Greak letters

γ	Dimensionless Curvature
δ	Dimensionless slug thickness
λ	Bubble formation wavelength
μ	Viscosity
σ	Interfacial tension